Received: 25 January 2023 | Revised: 24 March 2023 | Accepted: 5 April 2023

DOI: 10.1002/bkcs.12709

COMMUNICATION

BKCS BULLETIN OF THE KOREAN CHEMICAL SOCIETY

Mechanochemical synthesis and interfacial engineering of photothermal polymer composites for solar-driven water evaporation

Jihyo Kim[1] | Dongjun Lee[1] | Wansu Cho[1] | Beomjoo Yang[2] | Jongwon Jung[2] | Chiyoung Park[1]

[1]Energy Science and Engineering, Daegu Gyeongbuk Institute of Science & Technology, Daegu, Republic of Korea

[2]School of Civil Engineering, Chungbuk National University, Cheongju-si, Republic of Korea

Correspondence
Chiyoung Park, Energy Science and Engineering, Daegu Gyeongbuk Institute of Science & Technology, 333, Techno jungang-daero, Hyeonpung-eup, Dalseong-gun, Daegu, Republic of Korea.
Email: parkcy@dgist.ac.kr

Funding information
Korean Government, Grant/Award Number: 2022R1A4A3029737

Abstract

Freshwater generation has been extensively studied to address the global freshwater scarcity issue, although designing a simple, inexpensive system with high efficiency and sustainability is complicated. Solar-driven water evaporation is a promising, highly efficient water purification strategy. This paper reports the synthesis of a hydrophilic conductive polymer and its carbon nanotube (CNT) composites for efficient solar-driven water evaporation via a quick mechanochemical process. Doped polydiphenylamine (PD) and its CNT composites were obtained by the simple grinding of an inexpensive eutectic-phase monomer with oxidants, doping agents, and oxidized CNTs. The obtained composites exhibited high photothermal efficiency (89.9%) and water evaporation rate (1.41 kg m^{-2} h^{-1}) under 1 sun irradiation. Dual doping and introducing oxidized CNTs into PD enhanced the wettability, photothermal efficiency, and water evaporation performance. This study provides an effective strategy for the fast and facile fabrication of photothermal membranes for solar-driven freshwater generation.

KEYWORDS
conductive polymer, mechanochemical, membrane, photothermal, solar-driven water evaporation

INTRODUCTION

Although 70% of the Earth is covered by water, freshwater, which is essential for sustaining human life, is scarce. Approximately 60% of the global population (4.0 billion people) faces freshwater shortages for about a month in a year.[1] Ever since the scarcity of freshwater became a global issue, methods such as reverse osmosis,[2-4] distillation of seawater,[5-7] purification of polluted water,[8] and capture of moisture in air with absorbents have been developed to generate fresh water.[9,10] Solar-driven water evaporation using photothermal materials has attracted considerable attention in recent years for its potential application in addressing the crisis of clean water,[11-16] as this method relies solely on sunlight.[17] As solar energy is unlimited, powerful, and free, this system is almost sustainable.

To evaporate water efficiently, photothermal materials with high light absorption, low heat conductivity, extremely high light-to-heat conversion, and adequate wettability have been explored.[18-21] Photothermal materials can be classified as follows: metals and metal oxides,[22-25] carbon-based materials,[26-30] inorganic semiconductors,[31,32] and polymers.[33-35] Although many of these materials exhibit adequate evaporation efficiency, achieving a material possessing all of the previously reported properties is still challenging.

In particular, conductive polymers have been reported as excellent candidates because they are inexpensive and possess excellent efficiency and solar-to-heat conversion efficiency.[36] Polyaniline (PANI) and polypyrrole (PPy) are the most well-known conductive polymers exhibiting photothermal effects. PANI has shown excellent heating properties and can reach a temperature close to the boiling point of water.[37] Consequently, PANI and its various composites have been investigated, and their photothermal conversion efficiencies have been correlated with their doping states.[38]

Our group recently reported the mechanochemical synthesis of polydiphenylamine (PD) via simple grinding with a eutectic liquid (EL) consisting of diphenylamine (DPA), a benzophenone (BP) mixture, and an oxidant (ammonium persulfate, APS).[39] Prior to this study, our group demonstrated the facile dispersion of carbon nanotubes (CNTs) and commercial polymer-CNT composites using EL.[40] In previous studies, an electrically healable strain sensor was developed via the one-pot fabrication of PD-CNT composites by simple grinding.[41,42] Considering the structure of PD, which is similar to that of PANI, this simple polymerization of PD has great synergistic potential for the low-cost development of photothermal materials with high energy conversion efficiency.

This paper reports the facile mechanochemical processing of photothermal polymer-CNT composites using EL for efficient solar-driven water evaporation. Synthesized dual-doped PD (DD-PD) showed excellent solar-thermal conversion efficiency (85.7%) and temperature (93.4 °C) within 10 min under 1 sun irradiation. Under the same condition, DD-PD/CNT exhibited the highest solar-thermal conversion efficiency (89.9%) and temperature (97.6 °C). Dual doping and simply adding oxidants during mechanosynthesis helped modify the nature of PD from hydrophobic to hydrophilic and increased the water evaporation rate, resulting in excellent photothermal polymers with a wide light absorption range and high photothermal efficiency. Further, owing to the good affinity between the EL and CNT surface, we successfully fabricated hydrophilic conductive polymer-CNT composites (with a high water evaporation rate of ∼1.41 kg m^{-2} h^{-1}) by simply adding oxidized CNTs during synthesis.

RESULTS AND DISCUSSION

The mechanochemical synthesis of robust aromatic skeletal structures with polar functional groups might be beneficial for an efficient solar-driven water evaporation. In fact, many of the methods employed to fabricate photothermal membranes require tedious and solution-based processing. Consequently, solventless processes are preferred. Our group has previously reported that the mechanical grinding of the EL of DPA (mp = 50–53 °C, surface tension $\gamma = 39.3$ mJ m^{-2} at 60 °C) and BP (mp = 47–51 °C, $\gamma = 45.1$ mJ m^{-2} at 20 °C) can induce oxidative polymerization in the presence of APS.[39] Upon grinding at room temperature, the doping agents (phytic acid [PA] and HCl) instantly initiate polymerization and then become dark green colored viscous prepolymers (Figure 1). Furthermore, the simple addition of oxidized CNTs during grinding enabled the successful synthesis of hydrophilic conductive polymer-CNT composites (0.6 wt% CNT). The Fourier transform infrared spectra (FT-IR) revealed the characteristic peaks of PD (Figure S2). The bands at 3390 and 1595 cm^{-1} were attributed to the N—H stretching and bending of the secondary amine, respectively. The bands at 1500 and 1317 cm^{-1} were attributed to the C—C multiple bond stretching mode of the benzene ring and the C—N stretching mode of the aromatic secondary amine, respectively.

To prepare the membrane for solar-driven water evaporation, the polymers and composites were dispersed in ethanol, and then coated onto a hydrophilic PVDF membrane. The morphology of CNT, coated PDs, and DD-PD/CNTs on the supporting membrane plane surface was observed using field-emission scanning electron microscopy (FE-SEM). The rigid character of PD, constructed entirely with aromatic rings without any alkyl chains, contributed to the rough morphology of the DD-PD/CNT composite (Figure S3). Despite its rough surface, DD-PD/CNT successfully covered the PVDF membrane, and we observed CNT bundles evenly distributed throughout the entire DD-PD/CNT area, both in-plane and out-of-plane (as shown in Figure S4). Based on these findings, it is highly likely that the CNTs were uniformly dispersed in the DD-PD/CNT composite material, and that the dispersed CNT bundles in the polymer body acted as bridges between adjacent PD domains.

The wettability of each coated membrane surface was characterized by the contact angle test. The non-doped PD shows a high contact angle with a water drop without being absorbed into the polymer even after 5 min (Figure 2a), thus indicating the hydrophobic nature of PD. Despite the distribution of periodic secondary amines in the backbone of PD, the conjugated aromatic chain rendered the hydrophobicity to PD. As expected, doping with the conductive polymer increased the hydrophilicity of the polymers and decreased the contact angles. The D-PD and DD-PD show contact angles of 79.4° and 67.6°, respectively (Figure 2b,c). Additional doping of D-PD with HCl resulted in faster water absorption (20 s), whereas D-PD required 30 s to fully absorb the water drop under the same conditions. Among the samples, DD-PD/CNT shows the smallest contact angle (41.2°) and the fastest water drop absorption (15 s) (Figure 2d). It was thus confirmed that doping and the introduction of oxidized CNTs enhanced the wettability of the material.

The increased conductance and light absorption observed in DD-PD/CNT compared to DD-PD can be attributed to the presence of CNTs. DD-PD exhibited a conductance of 9.8×10^{-8} S, while the conductance of DD-PD/CNT was 1.53×10^{-7} S (Figure S5). Figure 3a shows the UV–vis–NIR spectroscopy results of PVDF/PDs and PVDF/DD-PD/CNT. Both membrane types demonstrated outstanding light absorption (>96%) within the 350–1300 nm wavelength range. PD, D-PD, and DD-PD displayed a slight decline in absorption between 500 and 700 nm, with the minimum absorption occurring at around 560 nm, which corresponds to the green color range in visible light. This observation can be explained by the fact that all PDs used in this study exhibited a greenish color. In contrast, DD-PD/CNT had the highest absorption rate (97.5%) among all samples within the

studied wavelength range. Owing to their high absorption rate over a wide range of wavelengths, PVDF/PDs and PVDF/DD-PD/CNT showed extremely high rates of photothermal temperature changes (Figure 3b). Under 1 sun irradiation (1 kW m^{-2}), the dry non-coated PVDF membrane exhibited the highest surface temperature of approximately 34 °C. Surprisingly, under the same irradiation conditions, dry PVDF/PD, PVDF/D-PD, and PVDF/DD-PD were heated to 81.7, 92, and 93.4 °C, respectively (Figure 3b,c). PVDF/DD-PD/CNT exhibited the highest temperature under sunlight (97.6 °C) among all photothermal membranes. The doping of PD not only enhanced the wettability, but also resulted in a higher temperature change under sunlight.

For solar-driven water evaporation, a customized device was assembled using photothermal membranes. The melamine foam was used to fix the membranes, and a cellulose filter steadily supplied water to the membranes. The photothermal membranes became wet upon their assembly on the device, and the surface temperature changes under sunlight decreased due to heat dissipation by the water molecules on the membranes (Figure 4a). Under wet conditions, PVDF/D-PD exhibited a temperature of 43.4 °C, which was slightly lower than those of PVDF/DD-PD and PVDF/DD-PD/CNT (45.8 and 46.7 °C, respectively). Considering that the non-coated PVDF membrane showed a temperature of 33 °C, all the coated membranes showed a temperature higher by 10 °C under wet conditions (Figure 4b). This difference resulted in a much larger difference in water evaporation under 1 sun irradiation (Figure 4c). The coated membranes recorded water evaporation of more than 1.2 kg m^{-2} h^{-1}, which was almost 2.5 times higher than that of the non-coated PVDF membrane (0.41 kg m^{-2} h^{-1}). It was thus confirmed that the water evaporation rate increased in the following order: PVDF/PD, PVDF/D-PD, PVDF/DD-PD, and PVDF/DD-PD/CNT having values of 1.24, 1.24, 1.34, and 1.41 kg m^{-2} h^{-1}, respectively. This is in accordance with the water wettability and photothermal heat generation test results. It was thus concluded that doping and the introduction of oxidized CNTs into PD increased the water evaporation rate under light irradiation. The PVDF/DD-PD/CNT displayed a seawater evaporation rate of 1.11 kg m^{-2} h^{-1} under 1 sun irradiation (Figure S6). This reduction in evaporation rate is likely due to the presence of salts such as NaCl, which exhibit strong electrostatic interactions with water molecules, restricting their movement and increasing the enthalpy of water evaporation, ultimately decreasing the evaporation rate. These results are consistent with findings from previous studies.[43-45]

We evaluated functional group changes using FT-IR before and after exposing the oxidized CNT to 100 °C for 6 h (as shown in Figure S7). Our results indicated a slight decrease in C—O peak intensity at 1240 cm^{-1}, which raised concerns about the thermal stability of CNT. Interestingly, we found that the water evaporation rate remained constant at 1.32 kg m^{-2} h^{-1} throughout

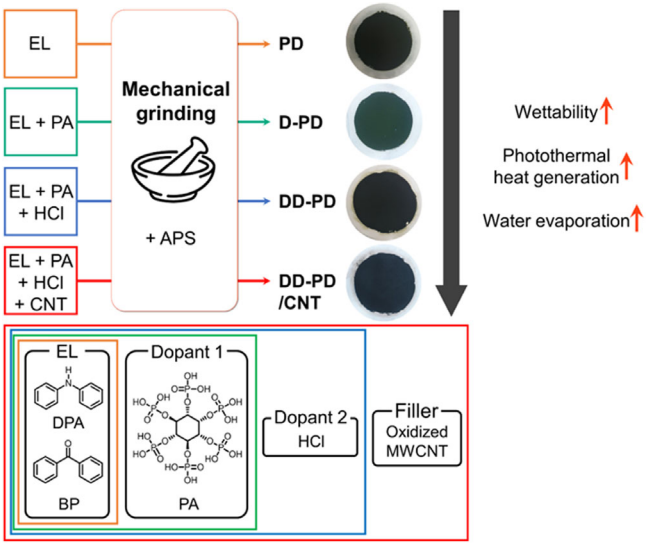

FIGURE 1 One-pot mechanochemical synthesis of PDs and DD-PD/CNT.

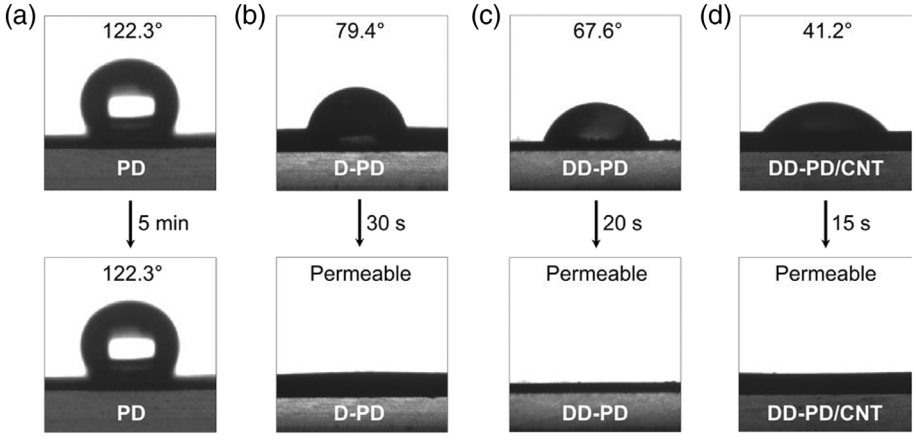

FIGURE 2 Snapshots of water droplets on (a) PD, (b) D-PD, (c) DD-PD, and (d) DD-PD/CNT.

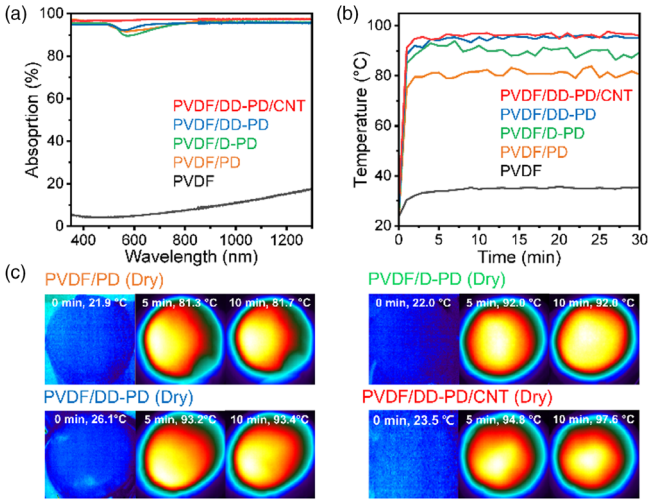

FIGURE 3 (a) Absorption spectra of PVDF, PVDF/PD, PVDF/D-PD, PVDF/DD-PD, and PVDF/DD-PD/CNT. (b) Photothermal heat generation of PVDF, PVDF/PD, PVDF/D-PD, PVDF/DD-PD, and PVDF/DD-PD/CNT in dry conditions under 1 sun irradiation. (c) Infrared thermal images of PVDF/PD, PVDF/D-PD, PVDF/DD-PD, and PVDF/DD-PD/CNT in dry conditions under 1 sun irradiation.

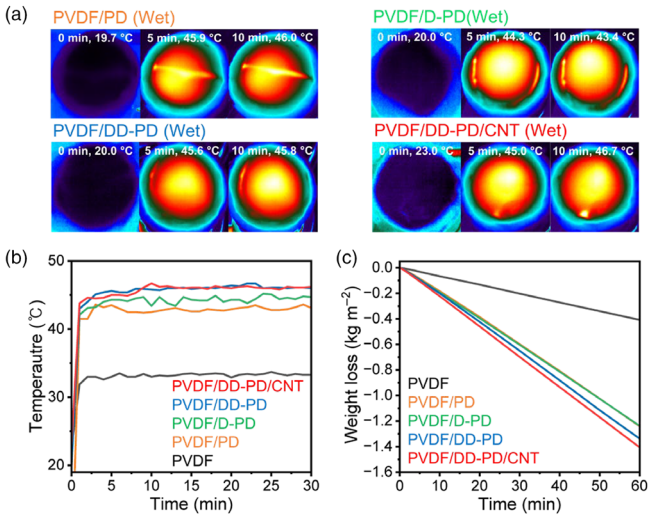

FIGURE 4 (a) Infrared thermal images of PVDF/PD, PVDF/D-PD, PVDF/DD-PD, and PVDF/DD-PD/CNT in wet conditions under 1 sun irradiation. (b) Time-dependent temperature changes of PVDF, PVDF/PD, PVDF/D-PD, PVDF/DD-PD, and PVDF/DD-PD/CNT in wet conditions under 1 sun irradiation. (c) Solar vapor generation performance of PVDF, PVDF/PD, PVDF/D-PD, PVDF/DD-PD, and PVDF/DD-PD/CNT under sunlight (AM 1.5G).

the entire duration of the experiment (as shown in Figure S8). Although we observed a decrease in the intensity of the C—O peak in the oxidized CNT, our results indicate that this instability did not have a significant effect on the efficiency of our system for water evaporation.

The solar-to-heat conversion efficiency is a key factor in the photothermal water evaporation and allows an evaluation of the actual energy conversion efficiency (η), which can be calculated using Equation (1).[46,47]

$$\eta = \frac{\dot{m} h_{lv}}{q} \times 100\%, \quad (1)$$

where $\dot{m}$ is the evaporation rate of water under steady-state conditions (kg m^{-2} s^{-1}), q is the intensity of the incoming solar irradiation, and h_{lv} corresponds to the total heat enthalpy of the liquid–vapor phase change including sensible and latent heat enthalpy, which can be calculated according to Equation (2):

$$h_{lv} = \lambda_{lv} + C_p \Delta T, \quad (2)$$

where λ_{lv} is the latent heat of vaporization of water at atmospheric pressure given as 2257 kJ kg^{-1}. C_p is the specific heat capacity of water (4.2 kJ kg^{-1} K^{-1}) and ΔT is the temperature rise of the water. The calculated solar-to-heat conversion efficiencies of PVDF/PD, PVDF/D-PD, PVDF/DD-PD, and PVDF/DD-PD/CNT were 78.2%, 79.0%, 85.7%, and 89.9%, respectively.

In order to identify the most effective dispersion amount of CNTs for optimal efficiency, various contents of CNTs (0.1, 0.6, and 1.2 wt%) were tested in the composite, and their corresponding solar-to-heat conversion efficiencies were calculated. The findings of our study demonstrated that the composites containing 0.1, 0.6, and 1.2 wt% of CNTs exhibited solar-to-heat conversion efficiencies of 77.2%, 89.9%, and 72.6%, respectively. These results suggest that various factors, including CNT dispersion, the ratio of polymer-to-CNT, and other interfacial effects, may have contributed to the observed outcomes.[34,35,37,48]

CONCLUSION

Solar-driven water evaporation is among the most promising methods for resolving the issue of freshwater scarcity owing to its high sustainability and low cost. This paper reported the mechanochemical synthesis of hydrophilic conductive polymers and their CNT composites for highly efficient solar-driven evaporation of water via fast and simple grinding. The doped conductive polymer-CNT composite exhibited excellent solar-to-heat conversion efficiency (89.9%) and could be heated up to 97.6 °C under 1 sun irradiation. Additional doping and the introduction of hydrophilic CNTs into the conductive polymer successfully enhanced the water wettability and photothermal heating performance. This study provides a facile, fast, and effective strategy for the synthesis of conductive polymer-based photothermal membranes via a low-energy process for solar-driven water evaporation.

ACKNOWLEDGMENTS

This work was supported by a National Research Foundation of Korea (NRF) grant, funded by the Korean Government (2022R1A4A3029737).

ORCID

Jihyo Kim https://orcid.org/0000-0003-3260-3108
Dongjun Lee https://orcid.org/0000-0002-5260-5250
Wansu Cho https://orcid.org/0000-0003-4037-0965
Beomjoo Yang https://orcid.org/0000-0002-2675-9774
Jongwon Jung https://orcid.org/0000-0001-9954-4232
Chiyoung Park https://orcid.org/0000-0002-6435-7004

REFERENCES

[1] M. M. Mekonnen, A. Y. Hoekstra, *Sci. Adv.* **2016**, *2*, e1500323.
[2] M. R. Islam, P. Khurana, P. Srikrishnarka, A. Nagar, M. Jash, S. K. Jenifer, M. A. Ganayee, M. Kumar, T. Pradeep, *Adv. Mater. Interfaces* **2021**, *8*, 2100533.
[3] Z. Jiang, S. Karan, A. G. Livingston, *Adv. Mater.* **2018**, *30*, 1705973.
[4] Y. Yao, P. Zhang, C. Jiang, R. M. DuChanois, X. Zhang, M. Elimelech, *Nat. Sustain.* **2021**, *4*, 138.
[5] X. Jiang, Y. Shao, J. Li, M. Wu, Y. Niu, X. Ruan, X. Yan, X. Li, G. He, *ACS Nano* **2020**, *14*, 17376.
[6] W. Wang, Y. Shi, C. Zhang, S. Hong, L. Shi, J. Chang, R. Li, Y. Jin, C. Ong, S. Zhuo, P. Wang, *Nat. Commun.* **2019**, *10*, 3012.
[7] S. Zhao, C. Jiang, J. Fan, S. Hong, P. Mei, R. Yao, Y. Liu, S. Zhang, H. Li, H. Zhang, C. Sun, Z. Guo, P. Shao, Y. Zhu, J. Zhang, L. Guo, Y. Ma, J. Zhang, X. Feng, F. Wang, H. Wu, B. Wang, *Nat. Mater.* **2021**, *20*, 1551.
[8] A. E. Kojo, W. Cho, C. Park, *J. Ind. Eng. Chem.* **2022**, *116*, 250.
[9] H. Kim, S. Yang, S. R. Rao, S. Narayanan, E. A. Kapustin, H. Furukawa, A. S. Umans, O. M. Yaghi, E. N. Wang, *Science* **2017**, *356*, 430.
[10] F. Zhao, X. Zhou, Y. Liu, Y. Shi, Y. Dai, G. Yu, *Adv. Mater.* **2019**, *31*, 1806446.
[11] W. Cho, D. Lee, G. Choi, J. Kim, A. E. Kojo, C. Park, *Adv. Mater.* **2022**, *34*, 2206982.
[12] J. Deng, S. Xiao, B. Wang, Q. Li, G. Li, D. Zhang, H. Li, A. C. S. Appl, *Mater. Interfaces* **2020**, *12*, 51537.
[13] Y. Peng, X. Wei, Y. Wang, W. Li, S. Zhang, J. Jin, *ACS Nano* **2022**, *16*, 8329.
[14] D. Qi, Y. Liu, Y. Liu, Z. Liu, Y. Luo, H. Xu, X. Zhou, J. Zhang, H. Yang, W. Wang, X. Chen, *Adv. Mater.* **2020**, *32*, 2004401.
[15] L. Shi, Y. Shi, S. Zhou, C. Zhang, Y. Aldrees, S. Aleid, P. Wang, *Nano Energy* **2019**, *60*, 222.
[16] P. Zhang, F. Zhao, W. Shi, H. Lu, X. Zhou, Y. Guo, G. Yu, *Adv. Mater.* **2022**, *34*, 2110548.
[17] C. Chen, Y. Kuang, L. Hu, *Joule* **2019**, *3*, 683.
[18] Y. Chen, Y. Wang, J. Xu, M. R. I. Raihan, B. Guo, G. Yang, M. Li, H. Bao, H. Xu, *Sol. RRL* **2022**, *6*, 2200202.
[19] D. Hao, Y. Yang, B. Xu, Z. Cai, *ACS Sustainable Chem. Eng.* **2018**, *6*, 10789.
[20] R. Zhang, Y. Zhou, B. Xiang, X. Zeng, Y. Luo, X. Meng, S. Tang, *Adv. Mater. Interfaces* **2021**, *8*, 2101160.
[21] F. Zhao, Y. Guo, X. Zhou, W. Shi, G. Yu, *Nat. Rev. Mater.* **2020**, *5*, 388.
[22] C. Kim, Y. Ryu, D. Shin, A. M. Urbas, K. Kim, *Appl. Surf. Sci.* **2020**, *517*, 146177.
[23] P. G. Struchalin, H. Thon, D. M. Kuzmenkov, K. V. Kutsenko, P. Kosinski, B. V. Balakin, *Int. J. Heat Mass Transfer* **2020**, *158*, 119987.
[24] M. N. Biutty, M. Zakia, S. I. Yoo, *Bull. Korean Chem. Soc.* **2020**, *41*, 1033.
[25] J. W. Ha, *Bull. Korean Chem. Soc.* **2015**, *36*, 2413.
[26] G. Ni, N. Miljkovic, H. Ghasemi, X. Huang, S. V. Boriskina, C.-T. Lin, J. Wang, Y. Xu, M. M. Rahman, T. Zhang, G. Chen, *Nano Energy* **2015**, *17*, 290.
[27] L. Shi, Y. Wang, L. Zhang, P. Wang, *J. Mater. Chem. A* **2017**, *5*, 16212.
[28] P. Zhang, J. Li, L. Lv, Y. Zhao, Y. Zhao, L. Qu, *ACS Nano* **2017**, *11*, 5087.
[29] L. Zhu, M. Gao, C. K. N. Peh, X. Wang, G. W. Ho, *Adv. Energy Mater.* **2018**, *8*, 1702149.
[30] L. Zhu, T. Ding, M. Gao, C. K. N. Peh, X. Wang, G. W. Ho, *Adv. Energy Mater.* **2019**, *9*, 1900250.
[31] X.-P. Li, X. Li, H. Li, Y. Zhao, J. Wu, S. Yan, Z.-Z. Yu, *Adv. Funct. Mater.* **2021**, *32*, 2110636.
[32] X. Zhao, X.-J. Zha, J.-H. Pu, L. Bai, R.-Y. Bao, Z.-Y. Liu, M.-B. Yang, W. Yang, *J. Mater. Chem. A* **2019**, *7*, 10446.
[33] S. M. Sajadi, N. Farokhnia, P. Irajizad, M. Hasnain, H. Ghasemi, *J. Mater. Chem. A* **2016**, *4*, 4700.
[34] Z. Zhu, P. Mu, Y. Fan, W. Bai, Z. Zhang, H. Sun, W. Liang, A. Li, *Eur. Polym. J.* **2020**, *126*, 109560.
[35] M. Tan, J. Wang, W. Song, J. Fang, X. Zhang, *J. Mater. Chem. A* **2019**, *7*, 1244.
[36] R. Djellabi, L. Noureen, V.-D. Dao, D. Meroni, E. Falletta, D. D. Dionysioiu, C. L. Bianchi, *Chem. Eng. J.* **2022**, *431*, 134024.
[37] Y. Zou, X. Chen, W. Guo, X. Liu, Y. Li, A. C. S. Appl, *Energy Mater.* **2020**, *3*, 2634.
[38] K. Wang, Z. Cheng, P. Li, Y. Zheng, Z. Liu, L. Cui, J. Xu, J. Liu, *J. Colloid Interface Sci.* **2021**, *581*, 504.
[39] W. Cho, C. Park, *Bull. Korean Chem. Soc.* **2019**, *40*, 914.
[40] C. B. Kim, K. B. Jeong, B. J. Yang, J.-W. Song, B.-C. Ku, S. Lee, S.-K. Lee, C. Park, *Angew. Chem. Int. Ed.* **2017**, *56*, 16180.
[41] J. Y. Yang, W. Cho, G. Choi, C. Park, *ChemElectroChem* **2020**, *7*, 3229.
[42] C. Park, S.-K. Lee, *ChemElectroChem* **2018**, *5*, 3589.
[43] G. Zhou, G. Jing, G. Xu, Q. Li, R. Huang, F. Li, H. Li, D. Wang, W. Chen, B. Z. Tang, *Nano Res.* **2022**, *15*, 6705.
[44] A. Wei, K. Cui, P. Wang, Y. Gu, X. Wang, X. Mu, Y. Tian, J. Zhou, Z. Sun, Y. Chen, J. Zhang, J. Liu, L. Miao, *Sol. RRL* **2021**, *5*, 2000782.
[45] Z. Yu, R. Gu, Y. Zhang, S. Guo, S. Cheng, S. C. Tan, *Nano Energy* **2022**, *98*, 107287.
[46] H. Li, Y. He, Y. Hu, X. Wang, A. C. S. Appl, *Mater. Interfaces* **2018**, *10*, 9362.
[47] Z. Tahir, S. Kim, F. Ullah, S. Lee, J.-H. Lee, N.-W. Park, M.-J. Seong, S.-K. Lee, T.-S. Ju, S. Park, J.-S. Bae, J. I. Jang, Y. S. Kim, A. C. S. Appl, *Mater. Interfaces* **2020**, *12*, 2490.
[48] W. Cho, C. Park, *J. Org. Chem.* **2019**, *8*, 1601.

SUPPORTING INFORMATION

Additional supporting information can be found online in the Supporting Information section at the end of this article.

How to cite this article: J. Kim, D. Lee, W. Cho, B. Yang, J. Jung, C. Park, *Bull. Korean Chem. Soc.* **2023**, *44*(8), 653. https://doi.org/10.1002/bkcs.12709